



# The Dominant Role of Brewer-Dobson Circulation on 17 O-Excess Variations in Snow Pits at Dome A, Antarctica

Hongxi Pang, Peng Zhang, Shuangye Wu, Jean Jouzel, Hans Christian Steen-larsen, Ke Liu, Wangbin Zhang, Jinhai Yu, Chunlei An, Deliang Chen, et al.

## ► To cite this version:

Hongxi Pang, Peng Zhang, Shuangye Wu, Jean Jouzel, Hans Christian Steen-larsen, et al.. The Dominant Role of Brewer-Dobson Circulation on 17 O-Excess Variations in Snow Pits at Dome A, Antarctica. *Journal of Geophysical Research: Atmospheres*, 2022, 127 (13), pp.e2022JD036559. 10.1029/2022jd036559 . hal-03738524

**HAL Id: hal-03738524**

**<https://hal.science/hal-03738524>**

Submitted on 26 Jul 2022

**HAL** is a multi-disciplinary open access archive for the deposit and dissemination of scientific research documents, whether they are published or not. The documents may come from teaching and research institutions in France or abroad, or from public or private research centers.

L'archive ouverte pluridisciplinaire **HAL**, est destinée au dépôt et à la diffusion de documents scientifiques de niveau recherche, publiés ou non, émanant des établissements d'enseignement et de recherche français ou étrangers, des laboratoires publics ou privés.

# JGR Atmospheres

## RESEARCH ARTICLE

10.1029/2022JD036559

### Key Points:

- The  $^{17}\text{O}$ -excess records in snow pits at Dome A show a significant correlation with the strength of the Brewer-Dobson circulation (BDC)
- Stronger BDC leads to more stratospheric water input over Antarctica and higher  $^{17}\text{O}$ -excess, and vice versa
- The  $^{17}\text{O}$ -excess records are also significantly correlated with the Southern Annular Mode, which dilutes the stratospheric water input

### Supporting Information:

Supporting Information may be found in the online version of this article.

### Correspondence to:

S. Hou and H. Pang,  
shuguihou@sjtu.edu.cn;  
hxpang@nju.edu.cn









### Citation:

Pang, H., Zhang, P., Wu, S., Jouzel, J., Steen-Larsen, H. C., Liu, K., et al. (2022). The dominant role of Brewer-Dobson circulation on  $^{17}\text{O}$ -excess variations in snow pits at Dome A, Antarctica. *Journal of Geophysical Research: Atmospheres*, 127, e2022JD036559. <https://doi.org/10.1029/2022JD036559>

Received 26 JAN 2022

Accepted 23 JUN 2022

## The Dominant Role of Brewer-Dobson Circulation on $^{17}\text{O}$ -Excess Variations in Snow Pits at Dome A, Antarctica

Hongxi Pang<sup>1</sup> , Peng Zhang<sup>2</sup> , Shuangye Wu<sup>3</sup> , Jean Jouzel<sup>4</sup>, Hans Christian Steen-Larsen<sup>5</sup> , Ke Liu<sup>1</sup>, Wangbin Zhang<sup>1</sup>, Jinhai Yu<sup>1</sup> , Chunlei An<sup>6</sup> , Deliang Chen<sup>2</sup> , and Shugui Hou<sup>1,7</sup> 

<sup>1</sup>Key Laboratory of Coast and Island Development of Ministry of Education, School of Geography and Ocean Science, Nanjing University, Nanjing, China, <sup>2</sup>Department of Earth Sciences, University of Gothenburg, Gothenburg, Sweden, <sup>3</sup>Department of Geology and Environmental Geosciences, University of Dayton, Dayton, OH, USA, <sup>4</sup>Laboratoire des Sciences du Climat et de l'Environnement, UMR8212, CEA-CNRS-UVSQ/IPSL, Gif-sur-Yvette, France, <sup>5</sup>Geophysical Institute, University of Bergen and Bjerknes Centre for Climate Research, Bergen, Norway, <sup>6</sup>Polar Research Institute of China, Shanghai, China, <sup>7</sup>School of Oceanography, Shanghai Jiao Tong University, Shanghai, China

**Abstract** Recent studies have suggested that water isotopologues in snow pits from remote East Antarctica can be influenced by the input of stratospheric water, which has anomalously high  $^{17}\text{O}$ -excess values. However, it remains unclear whether the  $^{17}\text{O}$ -excess records preserved in snow and ice from this region can be used to reconstruct stratosphere-troposphere exchange (STE). In this study, we present high-resolution  $^{17}\text{O}$ -excess records from two snow pits at Dome A, the highest point of the Antarctic ice sheet. The  $^{17}\text{O}$ -excess records show a significant positive correlation with the strength of the Brewer-Dobson circulation (BDC), the hemispheric-scale troposphere-stratosphere overturn circulation. Stronger BDC leads to more stratospheric water input over Antarctica and higher  $^{17}\text{O}$ -excess, and vice versa. In addition, the  $^{17}\text{O}$ -excess records also have a significant positive correlation with the Southern Annular Mode (SAM) index, because SAM modulates Antarctic precipitation, which has a dilution effect on the stratospheric water input. The  $^{17}\text{O}$ -excess records do not show significant correlations with local temperature and relative humidity in the moisture source region. These results suggest the dominant effect of BDC on  $^{17}\text{O}$ -excess and indicate the potential for using  $^{17}\text{O}$ -excess records in ice cores from remote sites in East Antarctica for reconstructing long-term variations of STE, and understanding their mechanisms and climate effects.

**Plain Language Summary** Previous studies suggest the influence of stratospheric water on  $^{17}\text{O}$ -excess variations in snow pits from the inland Ppateau of East Antarctica, and the potential for using ice-core  $^{17}\text{O}$ -excess to trace historical stratosphere-troposphere exchange. However, it remains unclear whether ice-core  $^{17}\text{O}$ -excess records from this remote part of East Antarctica can be used as a proxy for stratosphere-troposphere exchange. In this study, we presented high-resolution  $^{17}\text{O}$ -excess records from two snow pits at Dome A, the highest point of the Antarctic ice sheet. We found that the  $^{17}\text{O}$ -excess variations over the past several decades were mainly controlled by the strength of the Brewer-Dobson circulation. This discovery could open up an opportunity for new methods to reconstruct long-term variations of the Brewer-Dobson circulation.

## 1. Introduction

Previous studies have shown that the mass-independent fractionation of oxygen isotope (O-MIF) in the atmosphere can occur during photochemical reactions of ozone (Feilberg et al., 2013; Gao et al., 2002; Krankowsky et al., 2000; Mauersberger et al., 2001, 2003; Schueler et al., 1990; Thiemens, 1999, 2006). In the stratosphere, the O-MIF signal in ozone can be transferred to other oxygen-bearing radicals, such as hydroxyl (OH) and nitrogen oxides ( $\text{NO}_x$ ) (Lyons, 2001; Zahn et al., 2006), and in turn to stratospheric water vapor by  $\text{H}_2\text{O}$  recycling via OH and  $\text{NO}_x$  as well as methane oxidation via OH (Lyons, 2001, 2003; Zahn et al., 2006). These processes produce an anomalously high value of  $^{17}\text{O}$ -excess (defined as  $^{17}\text{O}\text{-excess} = \ln(\delta^{17}\text{O}+1) - 0.528\ln(\delta^{18}\text{O}+1)$ ,  $\delta^{17}\text{O}$  and  $\delta^{18}\text{O}$  stand for isotopic ratios of  $\text{H}_2^{17}\text{O}$  and  $\text{H}_2^{18}\text{O}$ ) in water vapor present in the middle and upper stratosphere up to  $\sim 30\text{‰}$  (30,000 per meg) (Lyons, 2003; Zahn et al., 2006). While the O-MIF in the atmosphere associated with photochemical reactions of ozone can significantly increase the fractionation line of oxygen isotopes, the tropospheric water, in contrast, has very low  $^{17}\text{O}$ -excess values because the isotopic fractionation processes (e.g., evaporation and condensation) are mass-dependent and can only alter the fractionation line of oxygen

isotopes slightly (i.e., the slope of linear relationship between  $\delta^{17}\text{O}$  and  $\delta^{18}\text{O}$ ). For instance, meteoric water has a mean  $^{17}\text{O}$ -excess value of  $\sim 37$  per meg (Luz & Barkan, 2010), and the precipitation  $^{17}\text{O}$ -excess over Antarctica would be reduced further due to kinetic isotopic fractionation that takes place when moisture becomes supersaturated at low temperatures (Angert et al., 2004; Landais et al., 2012; Miller, 2008, 2018; Pang et al., 2015; Risi et al., 2013). The large disparity between  $^{17}\text{O}$ -excess values in stratospheric and tropospheric water makes it a potentially useful tracer for stratosphere-troposphere transport driven by the Brewer-Dobson circulation (BDC).

The BDC is a global atmospheric circulation phenomenon that describes a hemispheric-scale troposphere-stratosphere overturn in which tropospheric air enters the stratosphere at tropical latitudes, moves poleward, and descends back into the troposphere at middle to high latitudes (Birner, 2010; Brewer, 1949; Butchart, 2014; Dobson, 1956; Fu et al., 2020; Holton et al., 1995; Iwasaki et al., 2009; Ploeger et al., 2019). Over inland regions of polar ice sheets, subsidence of air flow is notable especially in winter—as polar vortices form during polar nighttime due to the radiative cooling effects of the air and underlying ice sheet (Roscoe, 2004). In addition, the precipitation rate on inland polar ice sheets is extremely low due to the very low air temperature. As a consequence, snow deposited on inland regions of polar ice sheets, such as the inland plateau of East Antarctica, has highly favorable conditions to record an O-MIF signal in stratospheric water vapor.

Winkler et al. (2013) first reported that large interannual variations of  $^{17}\text{O}$ -excess in a snow pit at Vostok, Antarctica, were resulted from contamination by stratospheric water vapor. The finding suggests the possibility to reconstruct the history of the stratosphere-troposphere exchange (STE) by using  $^{17}\text{O}$ -excess records in ice cores collected from the inland regions of a polar ice sheet. However, this assertion has not yet been tested due to the paucity of  $^{17}\text{O}$ -excess data in snow pits from such localities and the uncertainty related to dating snow pits, which is caused by very low rates of accumulation, the lack of meteorological observations, the low reliability of reanalysis data in polar ice sheet regions, and possibly the notable precipitation dilution effect on the  $^{17}\text{O}$ -excess signal derived from stratospheric water.

Dome Argus (Dome A) is the highest point on the Antarctic ice sheet (4,093 m a.s.l.) and is located far inland on the East Antarctic Plateau (80°22'51"S, 77°27'23"E), being situated  $\sim 1,250$  km away from the coast. It is characterized by extreme climate conditions, with an annual mean temperature of  $-58.3^\circ\text{C}$  and a snow accumulation rate of  $23 \text{ mm a}^{-1}$  (Hou et al., 2007). In addition, Dome A is located in the core area of the Antarctic vortex, which makes it susceptible to stratospheric input (Ding et al., 2021). As a result, the  $^{17}\text{O}$ -excess in snow and ice at Dome A could be significantly influenced by the addition of stratospheric water. In this study, we conducted  $^{17}\text{O}$ -excess measurements on two snow pits at Dome A and aim to determine whether the  $^{17}\text{O}$ -excess in snow and ice at remote sites on the East Antarctic Plateau could be used to reconstruct historical variations of STE.

## 2. Materials and Methods

### 2.1. Snow Pit Analyses

A 3.0-m-deep snow pit was excavated at Dome A in January 2010 during the 26th Chinese National Antarctic Research Expedition (CHINARE-26), and a 4.5-m-deep snow pit was dug at Dome A in January 2016 during CHINARE-32. Thirty samples were collected from the 3.0-m-deep snow pit at a depth interval of 10 cm, whereas 174 samples were collected from the 4.5-m-deep snow pit at a depth interval of  $\sim 2.6$  cm. All samples were analyzed for  $\delta^{17}\text{O}$  and  $\delta^{18}\text{O}$  using a water fluorination method at the Laboratoire des Sciences du Climat et de l'Environnement (LSCE), France. The analytical uncertainty for  $^{17}\text{O}$ -excess is  $\sim 5$  per meg. In addition, the d-excess measurements performed on samples from both snow pits were conducted at the School of Geography and Ocean Science, Nanjing University (NJU), China, by a wavelength cavity ring-down spectroscopic technique (Model: Picarro L2120-i), which has an analytical uncertainty less than  $1.0\text{‰}$  (Li et al., 2020; Tang et al., 2015). An earlier study has determined the chronology of the 3.0-m-deep snow pit based on known ages for reference layers for the Pinatubo volcanic eruption (Philippines, June 1991), identified by the non-sea-salt sulfate peak and the 1963 radioactive nuclear bomb horizon, as determined by the maximum  $\beta$  activity (Hua et al., 2016). The 4.5-m-deep snow pit was dated based on reference layers for the Agung (Indonesia, March 1963), El Chichon (Mexico, late March and early April 1982), and Pinatubo volcanic eruptions, and the 1963 nuclear bomb horizon (Liu et al., 2021). The 3.0-m-deep pit was dated to cover 1964–2008, with a temporal resolution of between  $\sim 2$  years and  $\sim 3$  years, and the 4.5-m-deep pit was dated to cover 1950–2015, with a temporal resolution of less than 1 year.

## 2.2. Correlation Analysis Between the BDC and $^{17}\text{O}$ -Excess

We hypothesize that a stronger BDC would produce a higher  $^{17}\text{O}$ -excess in snow pits at Dome A because of the higher input rate of stratospheric water into the troposphere driven by the BDC, and vice versa. Therefore, the strength of the BDC must be quantified. In this study, the BDC is defined as a two-dimensional, equator-to-pole, and mean stratospheric mass circulation. We quantified the strength of the BDC by considering two net mass fluxes across the tropopause: (a) the net upward mass flux across the tropopause in the tropics ( $30^{\circ}\text{S}$  to  $30^{\circ}\text{N}$ ) and moving toward the south, hereafter referred to the strength of the upwelling branch of the BDC; and (b) the net downward mass flux across the tropopause in the Antarctic regions ( $60^{\circ}\text{S}$  to  $90^{\circ}\text{S}$ ), hereafter referred to the downwelling branch of the BDC. The mass flux across the tropopause was estimated based on the mass stream function (see Text S1 in Supporting Information S1). As the BDC is most prominent in winter (Butchart, 2014), our correlation analysis focused on the austral winter season (April to October). Additionally, as several years are needed for air to travel from low latitudes to high latitudes via the BDC (Garcia et al., 2011; Li et al., 2012; Ploeger et al., 2019), we calculated three separate correlations between  $^{17}\text{O}$ -excess and the strength of the upwelling branch of the BDC, which had lead times of 1, 2, and 3 years.

We performed analysis using several reanalysis data sets, including the NCEPv1 (Kalnay et al., 1996), ERA5 (Hersbach et al., 2018), ERA-Interim (Dee et al., 2011), ERA40 (Uppala et al., 2005), JRA55 (Kobayashi et al., 2015), and MERRA2 (Gelaro et al., 2017) (see details in Table S1 of Supporting Information S1); however, to reduce the uncertainty of these reanalysis data, we also calculated the correlation between  $^{17}\text{O}$ -excess and a composite of the BDC strength (composite reanalysis), which is defined as the mean of the standardized time series of the BDC strengths from all six of the reanalysis data sets. This standardized time series was determined using the Z-score method.

Dating uncertainty is difficult to evaluate, as the annual layer counting method cannot be used at Dome A due to its very low snow accumulation rate. To attenuate the influence of this dating uncertainty, a 5-year running average of  $^{17}\text{O}$ -excess data at Dome A and the BDC strength was used to calculate their correlations. It should be noted that we first got the BDC record with 1, 2, and 3 years of lead time from  $^{17}\text{O}$ -excess record and then calculated their correlations based on their 5-year running averages.

## 2.3. Multiple Linear Regression Analysis

In order to quantify the relative importance of different factors affecting  $^{17}\text{O}$ -excess at Dome A, we built a multiple linear regression model to examine how much of the variance in  $^{17}\text{O}$ -excess values can be explained by each of the controlling factors. We first built the model with all relevant variables used in this study, including the BDC upwelling, BDC downwelling, Southern Annular Mode (SAM) index, site temperature and precipitation, source region sea surface temperature (SST), and relative humidity. We then dropped nonsignificant variables one at a time until all remaining variables were statistically significant. We then established the relative importance of these variables based on their partial  $R^2$ , that is, the portion of the model  $R^2$  that was independently explained by each of the variables (Genizi, 1993).

## 2.4. Isotopic Simulations With a Rayleigh-Type Model

To understand the factors that control  $^{17}\text{O}$ -excess, we simulated the isotopic compositions ( $\delta^{18}\text{O}$ , d-excess, and  $^{17}\text{O}$ -excess) using a Rayleigh-type model mixed-cloud isotopic model (MCIM) (Ciais & Jouzel, 1994). This model was run from 1950 to 2015, forced by meteorological parameters in the moisture source region, such as SST and relative humidity (RH), and at the precipitation site, such as condensation temperature ( $T_c$ ). The forcing meteorological data were retrieved from the reanalysis data sets. We used the same MCIM parameterizations as documented by Pang et al. (2019), which successfully simulated the spatial distributions of d-excess and  $^{17}\text{O}$ -excess in surface snow along a transect (Syowa to Dome F) through the East Antarctica ice sheet. More details about the MCIM simulations are provided in the Supporting Information S1 (Text S2 in Supporting Information S1).

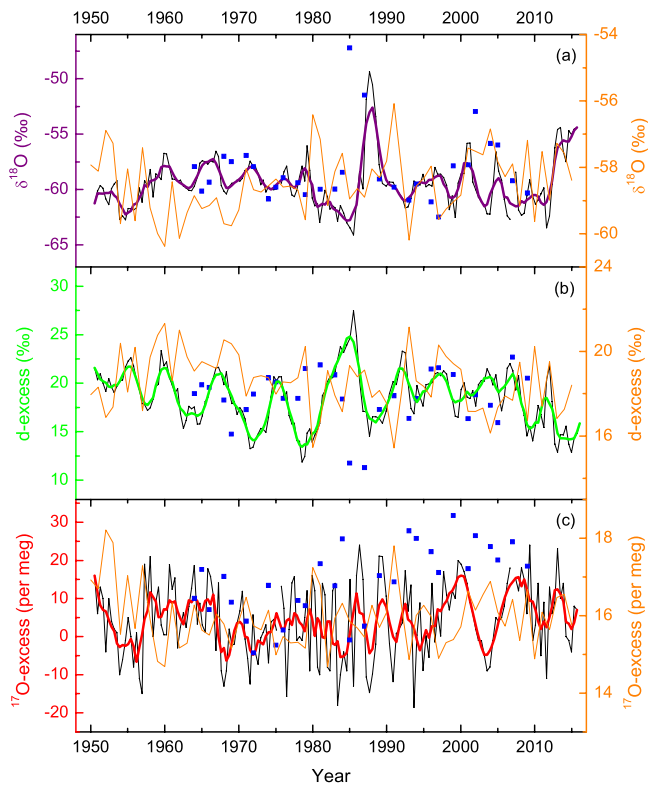


**Figure 1.** Measured and model mixed-cloud isotopic model (MCIM)-simulated  $\delta^{18}\text{O}$  (a), d-excess (b), and  $^{17}\text{O}$ -excess (c) values at Dome A over the past several decades. Thin black lines represent raw measurements of these parameters in the 4.5-m-deep snow pit of Dome A (174 samples) and associated thick lines correspond to their five-point moving averages. Thin orange lines represent annual values of  $\delta^{18}\text{O}$ , d-excess, and  $^{17}\text{O}$ -excess simulated by the MCIM. Raw measurements of  $\delta^{18}\text{O}$ , d-excess, and  $^{17}\text{O}$ -excess in the 3.0-m-deep snow pit of Dome A (30 samples; solid blue squares) are also presented for comparison.

### 3. Results

Figure 1 shows the time series of  $\delta^{18}\text{O}$ , d-excess, and  $^{17}\text{O}$ -excess in snow pits at Dome A, as well as their values simulated by the MCIM. Correlation coefficients between the strength of BDC and the  $^{17}\text{O}$ -excess record for the 4.5-m-deep snow pit are presented in Table 1. Positive correlations exist between the  $^{17}\text{O}$ -excess record and the strength of BDC upwelling with lead times of 1, 2, and 3 years. For most reanalysis data sets, this correlation is strongest for the BDC upwelling with a lead time of 3 years. It is noteworthy that the correlation is stronger for the composite of the BDC upwelling, as opposed to the BDC upwelling calculated using any individual reanalysis data set (Table 1; Figure 2). Compared with the BDC upwelling in the tropics, the  $^{17}\text{O}$ -excess correlation with the strength of the BDC downwelling in the Antarctic regions is much weaker, except for the MERRA2 data set (Table 1). In addition, there are no significant correlations between the strength of the BDC and either the  $\delta^{18}\text{O}$  or d-excess records.

### 4. Discussion

#### 4.1. Climatic Effects on $^{17}\text{O}$ -Excess

We compared the isotopic records ( $\delta^{18}\text{O}$ , d-excess, and  $^{17}\text{O}$ -excess) preserved in snow pits at Dome A with isotopic simulations using the MCIM (Figure 1). While the MCIM failed to simulate interannual variations of isotopic records at Dome A, this result is not unexpected, likely due to the following reasons: (a) the MCIM is a simple Rayleigh-type model that does not consider the actual moisture transport pathways and mixing of water vapor during transport; (b) there is uncertainty related to the forcing meteorological data in the model, which was retrieved from the reanalysis data sets; and (c) there is uncertainty associated with dating the Dome A snow pits. Nevertheless, the simulated  $^{17}\text{O}$ -excess shows a significant positive correlation with the simulated  $\delta^{18}\text{O}$  at Dome A (Figures 1a and 1c), suggesting the local temperature effect on  $^{17}\text{O}$ -excess due to kinetic isotopic fractionation that occurs when vapor condenses to ice crystals under supersaturated conditions at low temperatures (Angert et al., 2004; Risi et al., 2013; Schoenemann & Steig, 2016). This is confirmed by isotopic observations in snow and ice over

Antarctica (Landais et al., 2008, 2012; Pang et al., 2015; Schoenemann et al., 2014), which have a characteristic positive correlation between  $\delta^{18}\text{O}$  and  $^{17}\text{O}$ -excess. Despite this, there are no correlations between  $^{17}\text{O}$ -excess and  $\delta^{18}\text{O}$  in the snow pits at Dome A (Figures S1a and S1b in Supporting Information S1), suggesting that the local temperature effect on  $^{17}\text{O}$ -excess could be masked by other more dominant factors. Notably, a significant anticorrelation between  $\delta^{18}\text{O}$  and  $^{17}\text{O}$ -excess was observed in a 3.65-m-deep snow pit at Vostok by Winkler et al. (2013) (Figure S1c in Supporting Information S1), which suggests that the expected positive correlation between  $\delta^{18}\text{O}$  and  $^{17}\text{O}$ -excess is reversed by the input of stratospheric water vapor. However, this anticorrelation between  $\delta^{18}\text{O}$  and  $^{17}\text{O}$ -excess was absent from another 3.87-m-deep snow pit at Vostok (Figure S1d in Supporting Information S1) (Touzeau et al., 2016). The reason for such inconsistency is unclear, but the absence of an expected positive correlation between  $\delta^{18}\text{O}$  and  $^{17}\text{O}$ -excess at Dome A and Vostok at least suggests that local temperature is not a major factor for  $^{17}\text{O}$ -excess variations in those places.

In addition, no correlation was found between  $^{17}\text{O}$ -excess and relative humidity in the moisture source region of Dome A (Figure S2 in Supporting Information S1). However, this result may not be taken to preclude changes in relative humidity in the moisture source region influencing  $^{17}\text{O}$ -excess at Dome A, due to uncertainties related to relative humidity data retrieved from the reanalysis data and biases related to dating of samples from the snow pit. Nonetheless, the large interannual variation of  $^{17}\text{O}$ -excess ( $\sim 30$  per meg) recorded at Dome A (Figure 1c) would otherwise represent an unrealistic interannual variation of relative humidity in the moisture source region ( $\sim 30\%$ ), assuming that the simulated sensitivity of  $^{17}\text{O}$ -excess to relative humidity over the moisture source region is  $\sim 1$

**Table 1**

*Correlation Coefficients Between the  $^{17}\text{O}$ -Excess Record of the 4.5 m-Deep Snow Pit at Dome A and the Strength of the Brewer-Dobson Circulation (BDC) Upwelling in the Tropics, With Separate Lead Times of 1–3 Years, and the Strength of the BDC Downwelling in the Antarctic Region Over the Past Several Decades*

Reanalysis data set	BDC upwelling in the tropics			BDC downwelling in the Antarctic region	
	Lead time of 1 year	Lead time of 2 years	Lead time of 3 years	No lead time or lag	Period (AD)
NCEPv1	0.411 <sup>a</sup>	0.453 <sup>a</sup>	0.431 <sup>a</sup>	0.397 <sup>a</sup>	1950–2015
ERA5	0.556 <sup>a</sup>	0.581 <sup>a</sup>	0.623 <sup>a</sup>	0.049	1979–2015
ERA-Interim	0.371 <sup>b</sup>	0.339	0.340	0.296	1979–2015
ERA40	0.139	0.286	0.410 <sup>a</sup>	−0.031	1958–2001
JRA55	0.528 <sup>a</sup>	0.546 <sup>a</sup>	0.580 <sup>a</sup>	−0.305 <sup>b</sup>	1958–2015
MERRA2	0.180	0.388 <sup>b</sup>	0.548 <sup>a</sup>	0.555 <sup>a</sup>	1980–2015
Composite reanalysis	0.486 <sup>a</sup>	0.599 <sup>a</sup>	0.682 <sup>a</sup>	0.312 <sup>b</sup>	1950–2015

*Note.* Note that correlation coefficients were calculated using the 5-year running averages of  $^{17}\text{O}$ -excess and the strength of the BDC, due to uncertainty in dating snow pit at Dome A. The correlation between the strength of the BDC and the  $^{17}\text{O}$ -excess record of the 3.0-m-deep snow pit at Dome A was not calculated, given that the temporal resolution of this snow pit is relatively low.

<sup>a</sup>Correlation is significant at the 0.01 level ( $p < 0.01$ ). <sup>b</sup>Correlation is significant at the 0.05 level ( $p < 0.05$ ).

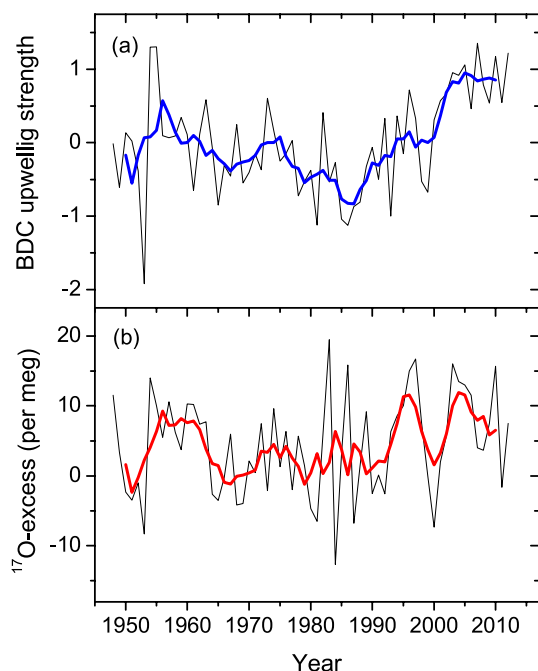


**Figure 2.** A comparison between the strength of the Brewer-Dobson circulation (BDC) upwelling in the tropics (a) and the  $^{17}\text{O}$ -excess record in the 4.5-m-deep snow pit at Dome A (b) over the past several decades. The BDC upwelling in the tropics precedes the  $^{17}\text{O}$ -excess records by three years. Thin lines are the annual time series and bold lines are the 5-year running averages. Note that the time series of the composite of the BDC upwelling, calculated using the Z-score method, was used to reduce the discrepancies between the different climate reanalysis data.

per meg/% (Landais et al., 2009; Risi et al., 2010; Winkler et al., 2012, 2013). These results therefore indicate that relative humidity in the moisture source region does not play a dominant role in controlling  $^{17}\text{O}$ -excess variations in snow pits at Dome A.

#### 4.2. Post-Deposition Effects on $^{17}\text{O}$ -Excess

In addition to climatic effects, we also analyzed the possible influence of postdepositional processes on  $^{17}\text{O}$ -excess, including blowing snow (Ekaykin et al., 2002), the isotopic exchange equilibrium between surface snow and near-surface vapor in-between precipitation events (Steen-Larsen et al., 2014), the isotopic diffusion of water molecules in the firn (Johnsen et al., 2000), and the moisture recycling associated with sublimation-condensation processes (Berkelhammer et al., 2016; Kopec et al., 2019). As the snow removed or redistributed by wind has the same effects on  $\delta^{17}\text{O}$  and  $\delta^{18}\text{O}$ , the blowing snow cannot modify snow  $^{17}\text{O}$ -excess. The isotopic exchange equilibrium between surface snow and near-surface vapor also cannot significantly change snow  $^{17}\text{O}$ -excess because  $^{17}\text{O}$ -excess is insensitive to temperature when isotopic equilibrium fractionation occurs. Although an isotopic model predicts the dampening of  $\delta^{18}\text{O}$  and  $^{17}\text{O}$ -excess due to the isotopic diffusion of water molecules in the firn, the isotopic fractionation in the firn cannot alter the positive correlation between  $\delta^{18}\text{O}$  and  $^{17}\text{O}$ -excess (Winkler et al., 2013). The lack of positive correlations between  $\delta^{18}\text{O}$  and  $^{17}\text{O}$ -excess at Vostok and Dome A (Figure S1 in Supporting Information S1) also suggests that the isotopic diffusion in the firn is not a major factor for the observed  $^{17}\text{O}$ -excess variations at Dome A (or Vostok). Winkler et al. (2013) suggested that the only mechanism that could lead to an anticorrelation between  $\delta^{18}\text{O}$  and  $^{17}\text{O}$ -excess at Vostok is the moisture recycling process, when surface snow is sublimated in summer at a relatively high temperature and the sublimated vapor is recondensed at a very low temperature. If this is the case, the amount of recondensation should be relatively high under low temperature (corresponding to a relatively strong BDC). As the recondensation lowers the  $^{17}\text{O}$ -excess, it

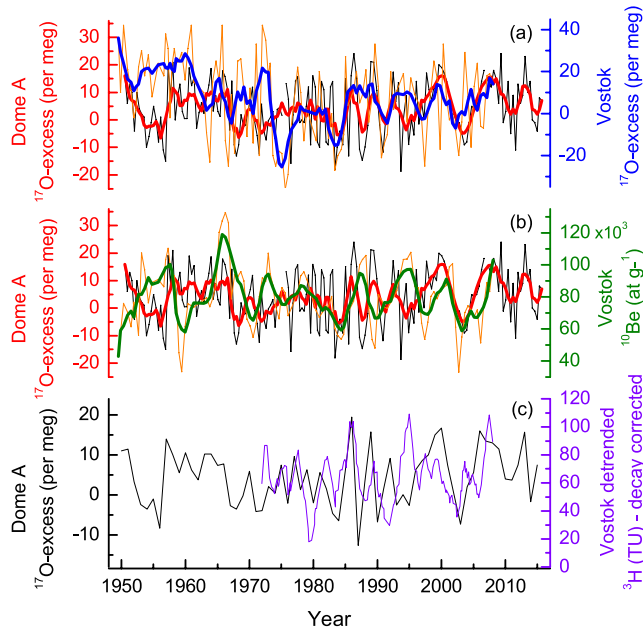


**Figure 3.** Comparisons of the  $^{17}\text{O}$ -excess record of the 4.5-m-deep snow pit at Dome A with records of  $^{17}\text{O}$ -excess (a),  $^{10}\text{Be}$  (b), and  $^3\text{H}$  (c) in snow pits at Vostok (Fourré et al., 2018; Winkler et al., 2013). Thin lines represent raw measurements of  $^{17}\text{O}$ -excess and  $^{10}\text{Be}$ , and thick lines correspond to their 5-point moving averages in (a) and (b). Annual means of  $^{17}\text{O}$ -excess at Dome A and  $^3\text{H}$  at Vostok are used for comparison in (c).

cannot account for the observed positive correlation between the strength of BDC and  $^{17}\text{O}$ -excess at Dome A. In summary, the post-deposition processes are not major factors for  $^{17}\text{O}$ -excess variations at Dome A.

#### 4.3. The Dominant Role of Brewer-Dobson Circulation on $^{17}\text{O}$ -Excess

A significant positive correlation between Dome A  $^{17}\text{O}$ -excess and the strength of the BDC upwelling in the tropics (Table 1 and Figure 2), alongside the lack of correlation between Dome A  $^{17}\text{O}$ -excess and  $\delta^{18}\text{O}$  (Figures S1a and S1b in Supporting Information S1) and relative humidity in the moisture source region (Figure S2 in Supporting Information S1), suggest that the strength of the BDC upwelling has strongly influenced  $^{17}\text{O}$ -excess variations at Dome A over the past several decades. Nevertheless, the  $^{17}\text{O}$ -excess correlation with the strength of BDC downwelling is very weak (Table 1), possibly due to annual variations of the latitudinal boundary of the BDC downwelling or the isentropic exchange of mass between the stratosphere and troposphere at middle to high latitudes, where tropopause folding occurs (Holton et al., 1995). We note that our model calculated the BDC downwelling strength based on a fixed latitudinal boundary. In addition, the reliability of reanalysis data over the tropical regions is likely better than that over the polar regions, where climate observations are relatively sparse. Because the mass flux driven by the BDC upwelling represents the global mass-transport capability of the BDC, we infer that a high mass flux driven by the BDC upwelling would lead to a high flux of stratospheric water into the troposphere over Antarctica, which in turn would produce high  $^{17}\text{O}$ -excess values in snow pits at Dome A, and vice versa. This inference is supported by the strong positive correlation between the mass flux and water flux driven by the BDC (Figure S3 in Supporting Information S1). The correlation between  $^{17}\text{O}$ -excess and

the BDC upwelling mass flux is stronger than that between  $^{17}\text{O}$ -excess and the BDC upwelling water flux (Table S2 in Supporting Information S1), as the former is more representative of the capability of BDC to transport water than the latter, because about half of the stratospheric water content is produced via H-abstraction from methane and other H-bearing species, such as  $\text{HO}_2$  and  $\text{HNO}_3$ , through the OH radical (Dessler et al., 1995; Lyons, 2001).

In order to further corroborate the dominant role of the BDC on  $^{17}\text{O}$ -excess variations at Dome A, we compared the  $^{17}\text{O}$ -excess record of the 4.5-m-deep snow pit at Dome A with other records of stratospheric tracers ( $^{17}\text{O}$ -excess,  $^{10}\text{Be}$ , and  $^3\text{H}$ ) in snow pits at Vostok (Figure 3) (Fourré et al., 2018; Winkler et al., 2013). Despite dating uncertainties, mostly related to the very low snow accumulation rate, the  $^{17}\text{O}$ -excess record at Dome A shows similar variations to  $^{17}\text{O}$ -excess (Figure 3a),  $^{10}\text{Be}$  (Figure 3b), and  $^3\text{H}$  (Figure 3c) records at Vostok since the mid-1970s at the interannual timescale (Fourré et al., 2018). For instance, the  $^{17}\text{O}$ -excess record at Dome A is significantly correlated with the  $^{17}\text{O}$ -excess record at Vostok over the period of 1976–2008 ( $r = 0.424$ ,  $p = 0.02$ ), and with the  $^3\text{H}$  record at Vostok since the 1970s ( $r = 0.297$ ,  $p = 0.07$ ). Although there is no significant correlation between the Dome A  $^{17}\text{O}$ -excess and Vostok  $^{10}\text{Be}$ , their variations are similar over the periods of mid-1970s to mid-1980s and late-1990s to 2008. We do not expect a good correlation between  $^{10}\text{Be}$  and  $^{17}\text{O}$ -excess, because in addition to stratospheric input, other factors, such as  $^{10}\text{Be}$  production, tropospheric transport, and dry or wet deposition (Heikkilä et al., 2013), also influence  $^{10}\text{Be}$  concentration at Vostok. The similarities are less before the mid-1970s, likely due to increasing uncertainty with snowpit chronologies and the increasing effect of diffusion in the firn with depth.

At decadal timescales, the  $^{17}\text{O}$ -excess record at Dome A shows similar variations to the  $^3\text{H}$  record at Vostok (Figures 4a and 4c), which correspond to solar Schwabe cycles (Figure 4a) (Fourré et al., 2018). In years featuring strong solar activity (e.g., many visible sunspots), ultraviolet heating of stratospheric ozone would increase the latitudinal temperature gradient between the tropics and the polar regions in the upper stratosphere, and so enhance westerly jets in the upper stratosphere over mid-latitude regions (Matthes et al., 2004; Shi et al., 2018). Strong westerly jets would prevent planetary waves propagating to the extratropical upper stratosphere, where the waves would break, and the weak wave forcing would produce a weak BDC, and vice versa

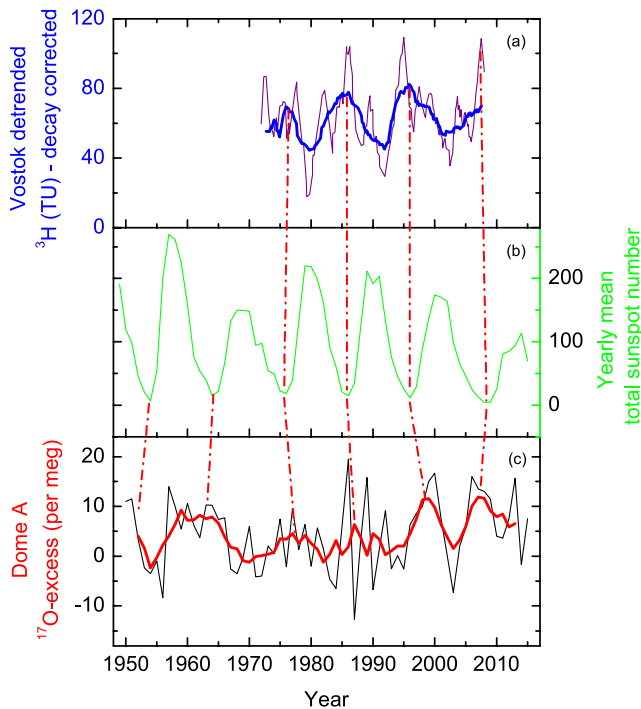


**Figure 4.** Comparisons of the  $^{17}\text{O}$ -excess record in the 4.5-m-deep snow pit at Dome A with the  $^3\text{H}$  record at Vostok (Fourré et al., 2018) and yearly mean total sunspot number (WDC-SILSO, Royal Observatory of Belgium, Brussels) at decadal timescales. Thin lines represent annual means and thick lines correspond to their 5-year running averages. Wiggle matching at decadal timescale, indicated by dash-dot lines, was used for comparison due to uncertainty associated with Dome A snow pit dating and strong decadal cycle of solar activity that can influence the BDC strength. It should be noted that the wiggle matching used here is subjective.

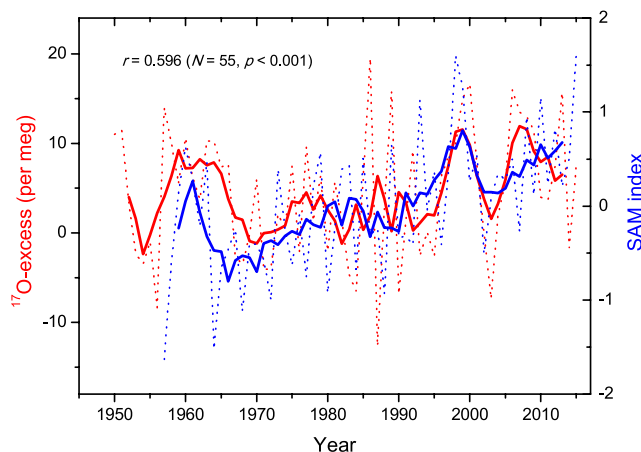


**Figure 5.** A comparison between the Southern Annular Mode (SAM) index and the  $^{17}\text{O}$ -excess record in the 4.5-m-deep snow pit at Dome A over the past several decades. Thin dot lines are annual means, bold lines are 5-year running averages, and  $r$  is the correlation coefficient between the 5-year running averages of  $^{17}\text{O}$ -excess and SAM index. An observation-based SAM index (Marshall, 2003) was used in this study.

(Butchart, 2014; Cohen et al., 2014; Holton et al., 1995). This mechanism explains why the  $^{17}\text{O}$ -excess record at Dome A shows anti-phase variations with the number of sunspots at a decadal timescale (Figures 4b and 4c).

#### 4.4. Precipitation Dilution Effect on $^{17}\text{O}$ -Excess

The  $^{17}\text{O}$ -excess record at Dome A also shows a significant positive correlation with the SAM index (Figure 5) (Marshall, 2003). Previous studies indicate that local temperature and precipitation over Antarctica are influenced by the SAM (Naik et al., 2010; Schneider et al., 2006), with low temperature and precipitation over Antarctica during the positive phase of the SAM, and vice versa. Low temperatures are favorable for more stratospheric moisture input, and low snow accumulation means less dilution of stratospheric water. Both conditions, which occur when the SAM index is high, would lead to high values of  $^{17}\text{O}$ -excess at Dome A. The opposite scenario is also true. High temperatures and high precipitation that occur during the negative phase of SAM would lead to low  $^{17}\text{O}$ -excess values. The dilution effect is also confirmed by a significant negative correlation between  $^{17}\text{O}$ -excess values and the amount of precipitation at Dome A (Figure S4 in Supporting Information S1). In fact, the positive correlation between  $^{17}\text{O}$ -excess and SAM further supports the influence of BDC on  $^{17}\text{O}$ -excess at Dome A.

We then used the multiple regression model to quantify the impact of different factors that control  $^{17}\text{O}$ -excess variations. From all variables with potential impact on  $^{17}\text{O}$ -excess, the final three statistically significant variables are included in the model: BDC upwelling, SAM index, and BDC downwelling. The three variables together could explain 58% of total variance in  $^{17}\text{O}$ -excess values. The most important variable is the BDC upwelling, which explains 32% of  $^{17}\text{O}$ -excess variance. SAM index explains 22%. The BDC downwelling explains an additional 4% of the  $^{17}\text{O}$ -excess variance. This analysis shows that  $^{17}\text{O}$ -excess at Dome A is primarily driven by BDC upwelling strength, but it is also significantly affected by the dilution effect modulated by SAM.

## 5. Conclusions and Future Prospects

We measured the triple oxygen isotopic composition of two snow pits at Dome A, the highest point of the Antarctic ice sheet.  $^{17}\text{O}$ -excess at Dome A shows a significant positive correlation with the strength of the BDC but no significant correlations with local temperature and relative humidity in the moisture source region over the past several decades. When the BDC is stronger, more stratospheric water is transported to Antarctic regions, which leads to higher  $^{17}\text{O}$ -excess at Dome A, and vice versa. These results suggest that  $^{17}\text{O}$ -excess variations at Dome A are mainly controlled by the strength of the BDC. In addition,  $^{17}\text{O}$ -excess variations at Dome A are also significantly affected by Antarctic precipitation, modulated by the SAM, because of dilution effect on  $^{17}\text{O}$ -excess. The finding may open up new possibilities to reconstruct long-term variations of BDC using ice-core  $^{17}\text{O}$ -excess records from interior Antarctica.

In order to effectively use ice core  $^{17}\text{O}$ -excess records to reconstruct historical behavior of the BDC, it is necessary to further quantify the influences of stratospheric water input on  $^{17}\text{O}$ -excess in snow and ice over remote Antarctica through precise measurements of  $^{17}\text{O}$ -excess in stratospheric water as well as developing a chemical climate model of the stratosphere that incorporates water isotopologues, including triple oxygen isotopes. This could be

achieved with the improvements of in situ spectroscopic measurements, such as a water isotope spectrometer based on optical feedback cavity-enhanced absorption (Kerstel et al., 2006). In addition, the signal of O-MIF in stratospheric water could be also acquired via spectroscopy by continuous near-surface measurements of isotopic compositions of water vapor during a stratospheric air intrusion (Galewsky & Samuels-Crow, 2014). Nonetheless, more and longer time series of  $^{17}\text{O}$ -excess records in ice cores from remote Antarctica are needed for potentially reconstructing long-term variations of the BDC.

## Data Availability Statement

The isotopic data from Dome A presented in the manuscript are available at <https://doi.org/10.5281/zenodo.6470612> (Pang et al., 2022). The NCEPv1 reanalysis data (Kalnay et al., 1996) are available at <https://psl.noaa.gov/data/gridded/data.ncep.reanalysis.html>. The ERA5 reanalysis data (Hersbach et al., 2018) are available at <https://cds.climate.copernicus.eu/cdsapp%23%21/dataset/reanalysis%2Dera5%2Dpressure%2Dlevels%3Ftab%3Doverview>. The ERA-Interim reanalysis data (Dee et al., 2011) are available at <https://www.ecmwf.int/en/forecasts/datasets/reanalysis-datasets/era-interim>. The ERA40 reanalysis data (Uppala et al., 2005) are available at <https://apps.ecmwf.int/datasets/data/era40-daily/levtype=sfc/>. The JRA55 reanalysis data (Kobayashi et al., 2015) are available at <https://rda.ucar.edu/datasets/ds628.1/>. The MERRA2 reanalysis data (Gelaro et al., 2017) are available at <https://disc.gsfc.nasa.gov/datasets?project=MERRA-2>. The Southern Annular Mode (SAM) index data (Marshall, 2003) are available at <https://legacy.bas.ac.uk/met/gjma/sam.html>. The sunspot number data (WDC-SILSO) are available at <https://wwwbis.sidc.be/silso/datafiles>.

## Acknowledgments

We thank all of the CHINARE-26 and CHINARE-32 scientists, technicians, and porters for their hard work in the field. We thank Amaelle Landais (LSCE) for the  $^{17}\text{O}$ -excess measurements and her constructive comments on this paper. We also thank Tongmei Wang for her advice on calculating the residual circulation. This work was jointly supported by the National Natural Science Foundation of China (41622605, 41830644, 91837102, 42021001), the Chinese Arctic and Antarctic Administration (CXPT2020012), the Priority Academic Program Development of Jiangsu Higher Education Institutions (PAPD), and the Swedish STINT (CH2019-8377).

## References

- Angert, A., Cappa, C. D., & DePaolo, D. J. (2004). Kinetic  $^{17}\text{O}$  effects in the hydrologic cycle: Indirect evidence and implications. *Geochimica et Cosmochimica Acta*, 68(17), 3487–3495. <https://doi.org/10.1016/j.gca.2004.02.010>
- Berkelhammer, M., Noone, D. C., Steen-Larsen, H. C., Bailey, A., Cox, C. J., O'Neill, M. S., et al. (2016). Surface-atmosphere decoupling limits accumulation at Summit, Greenland. *Science Advances*, 2(4), e1501704. <https://doi.org/10.1126/sciadv.1501704>
- Birner, T. (2010). Residual circulation and tropopause structure. *Journal of the Atmospheric Sciences*, 67(8), 2582–2600. <https://doi.org/10.1175/2010jas3287.1>
- Brewer, A. W. (1949). Evidence for a world circulation provided by the measurements of helium and water vapour distribution in the stratosphere. *Quarterly Journal of the Royal Meteorological Society*, 75(326), 351–3363. <https://doi.org/10.1002/qj.49707532603>
- Butchart, N. (2014). The Brewer-Dobson circulation. *Reviews of Geophysics*, 52(2), 157–184. <https://doi.org/10.1002/2013RG000448>
- Ciais, P., & Jouzel, J. (1994). Deuterium and oxygen 18 in precipitation: Isotopic model, including mixed cloud processes. *Journal of Geophysical Research*, D99(D8), 16793. <https://doi.org/10.1029/94jd00412>
- Cohen, N. Y., Gerber, E. P., & Bühler, O. (2014). What drives the Brewer-Dobson circulation? *Journal of the Atmospheric Sciences*, 71(10), 3837–3855. <https://doi.org/10.1175/jas-d-14-0021.1>
- Dee, D. P., Uppala, S. M., Simmons, A. J., Berrisford, P., Poli, P., Kobayashi, S., et al. (2011). The ERA-Interim reanalysis: Configuration and performance of the data assimilation system. *Quarterly Journal of the Royal Meteorological Society*, 137(656), 553–597. [Dataset]. <https://doi.org/10.1002/qj.828>
- Dessler, A. E., Hints, E. J., Weinstock, E. M., Anderson, J. G., & Chan, K. R. (1995). Mechanisms controlling water vapour in the lower stratosphere: "A tale of two stratospheres". *Journal of Geophysical Research*, 100(D11), 23167–23172. <https://doi.org/10.1029/95jd02455>
- Ding, M., Tian, B., Ashley, M. C. B., Putero, D., Zhu, Z., Wang, L., et al. (2021). Year-round record of near-surface ozone and  $\text{O}_3$  enhancement events (OEEs) at Dome A, East Antarctica. *Earth System Science Data*, 12(4), 3529–3544. <https://doi.org/10.5194/essd-12-3529-2020>
- Dobson, G. M. B. (1956). Origin and distribution of the polyatomic molecules in the atmosphere. In *Proceedings of royal society A-mathematical physical and engineering Sciences* (Vol. 236, pp. 187–193).
- Ekaykin, A. A., Lipenkov, V. Y., Barkov, N. I., Petit, J. R., & Masson-Delmotte, V. (2002). Spatial and temporal variability in isotope composition of recent snow in the vicinity of Vostok station, Antarctica: Implications for ice-core record interpretation. *Annals of Glaciology*, 35(1), 181–186. <https://doi.org/10.3189/172756402781816726>
- Feilberg, K. L., Wiegel, A. A., & Boering, K. A. (2013). Probing the unusual isotope effects in ozone formation: Bath gas and pressure dependence of the non-mass-dependent isotope enrichments in ozone. *Chemical Physics Letters*, 556, 1–8. <https://doi.org/10.1016/j.cplett.2012.10.038>
- Fourré, E., Landais, A., Cauquoin, A., Jeanbaptiste, P., & Petit, J. R. (2018). Tritium records to trace stratospheric moisture inputs in Antarctica. *Journal of Geophysical Research: Atmospheres*, 123(6), 3009–3018. <https://doi.org/10.1002/2018jd028304>
- Fu, Q., White, R. H., Wang, M., Alexander, B., Solomon, S., Gettelman, A., et al. (2020). The Brewer-Dobson circulation during the Last Glacial Maximum. *Geophysical Research Letters*, 47(5), e2019GL086271. <https://doi.org/10.1029/2019gl086271>
- Galewsky, J., & Samuels-Crow, K. (2014). Water vapor isotopic composition of a stratospheric air intrusion: Measurements from the Chajnantor Plateau, Chile. *Journal of Geophysical Research: Atmospheres*, 119(16), 9679–9691. <https://doi.org/10.1002/2014jd022047>
- Gao, Y. Q., Chen, W. C., & Marcus, R. A. (2002). A theoretical study of ozone isotopic effects using a modified ab initio potential energy surface. *Journal of Chemical Physics*, 117(4), 1536–1543. <https://doi.org/10.1063/1.1488577>
- García, R. R., Randel, W. J., & Kinnison, D. E. (2011). On the determination of age of air trends from atmospheric trace species. *Journal of the Atmospheric Sciences*, 68(1), 139–154. <https://doi.org/10.1175/2010jas3527.1>
- Gelaro, R., McCarty, W., Suárez, R., Todling, R., Molod, A., Takacs, L., et al. (2017). The modern-era retrospective analysis for research and applications, version 2 (MERRA-2). *Journal of Climate*, 30(14), 5419–5454. [Dataset]. <https://doi.org/10.1175/jcli-d-16-0758.1>
- Genizi, A. (1993). Decomposition of  $R^2$  in multiple regression with correlated regressors. *Statistica Sinica*, 3, 407–420.

- Heikkilä, U., Beer, J., Abreu, J. A., & Steinhilber, F. (2013). On the atmospheric transport and deposition of the cosmogenic radionuclides ( $^{10}\text{Be}$ ): A review. *Space Science Reviews*, 176(1–4), 321–332. <https://doi.org/10.1007/s11214-011-9838-0>
- Hersbach, H., Bell, B., Berrisford, P., Biavati, G., Horányi, A., Muñoz Sabater, J., et al. (2018). ERA5 hourly data on pressure levels from 1979 to present. Copernicus Climate Change Service (C3S) Climate Data Store (CDS). [Dataset]. <https://cds.climate.copernicus.eu/cdsapp%23%21/dataset/reanalysis%2Dera5%2Dpressure%2Dlevels%3Ftab%3DOverview>
- Holton, J. R., Haynes, P. H., McIntyre, P. H., Douglass, A. R., Rodd, R. B., & Pfister, L. (1995). Stratosphere-troposphere exchange. *Review of Geophysics*, 33(4), 403–439. <https://doi.org/10.1029/95rg02097>
- Hou, S., Li, Y., Xiao, C., & Ren, J. (2007). Recent accumulation rate at Dome A, Antarctica. *Chinese Science Bulletin*, 52(3), 428–431. <https://doi.org/10.1007/s11434-007-0041-3>
- Hua, R., Hou, S., Li, Y., Pang, H., Mayewski, P., Sneed, S., et al. (2016). Arsenic record from a 3 m snow pit at Dome Argus, Antarctica. *Antarctic Science*, 28(4), 305–312. <https://doi.org/10.1017/s0954102016000092>
- Iwasaki, T., Hamada, H., & Miyazaki, K. (2009). Comparisons of Brewer-Dobson circulations diagnosed from reanalyses. *Journal of the Meteorological Society of Japan*, 36(6), 997–1006. <https://doi.org/10.2151/jmsj.87.997>
- Johnsen, S. J., Clausen, H. B., Cuffey, K. M., Hoffmann, G., Schwander, J., & Creyts, T. (2000). Diffusion of stable isotopes in polar firn and ice: The isotope effect in firn diffusion. In T. Hondoh (Ed.), *PICR "physics of ice core records", institute of low temperature science* (pp. 121–140). Hokkaido University Press.
- Kalnay, E. M., Kanamitsu, M., Kistler, R., Collins, W., Leetmaa, A., Gandin, L., et al. (1996). The NCEP/NCAR 40-year reanalysis project. Bulletin of the American Meteorological Society, 77(3), 437–472. [Dataset]. [https://doi.org/10.1175/1520-0477\(1996\)077<0437:tnyrp>2.0.co;2](https://doi.org/10.1175/1520-0477(1996)077<0437:tnyrp>2.0.co;2)
- Kerstel, E. R. T., Iannone, R. Q., Chenevier, M., Jost, H. J., & Romanini, D. (2006). A water isotope ( $^2\text{H}$ ,  $^{17}\text{O}$ , and  $^{18}\text{O}$ ) spectrometer based on optical feedback cavity-enhanced absorption for in situ airborne applications. *Applied Physics B*, 85(2–3), 397–406. <https://doi.org/10.1007/s00340-006-2356-1>
- Kobayashi, S., Ota, Y., Harada, Y., Ebata, A., Moriya, M., Onoda, H., et al. (2015). The JRA-55 reanalysis: General specifications and basic characteristics. *Journal of the Meteorological Society of Japan*, 93(1), 5–48. [Dataset]. <https://doi.org/10.2151/jmsj.2015-001>
- Kopec, B. G., Feng, X., Posmentier, E. S., & Sonder, L. J. (2019). Seasonal deuterium excess variations of precipitation at Summit, Greenland, and their climatological significance. *Journal of Geophysical Research: Atmospheres*, 124(1), 72–91. <https://doi.org/10.1029/2018jd028750>
- Krankowsky, D., Lämmerzahl, P., & Mauersberger, K. (2000). Isotopic measurements of stratospheric ozone. *Geophysical Research Letters*, 27(17), 2593–2595. <https://doi.org/10.1029/2000gl011812>
- Landais, A., Barkan, E., & Luz, B. (2008). Record of  $\delta^{18}\text{O}$  and  $^{17}\text{O}$ -excess in ice from Vostok Antarctica during the last 150,000 years. *Geophysical Research Letters*, 35(2), L02709. <https://doi.org/10.1029/2007GL032096>
- Landais, A., Barkan, E., Vimeux, F., Masson-Delmotte, V., & Luz, B. (2009). Combined analysis of water stable isotopes ( $\text{H}_2^{16}\text{O}$ ,  $\text{H}_2^{17}\text{O}$ ,  $\text{H}_2^{18}\text{O}$ ,  $\text{HD}^{16}\text{O}$ ). In T. Hondoh (Ed.), *PICR "physics of ice-core records", institute of low temperature science* (pp. 315–327). Kokkaido University Press.
- Landais, A., Ekaykin, A., Barkan, E., Winkler, R., & Luz, B. (2012). Seasonal variations of  $^{17}\text{O}$ -excess and d-excess in snow precipitation at Vostok station, East Antarctica. *Journal of Glaciology*, 58(210), 725–733. <https://doi.org/10.3189/2012jog11j237>
- Li, F., Waugh, D. W., Douglass, A. R., Newman, P. A., Strahan, S. E., Ma, J., et al. (2012). Long-term changes in stratospheric age spectra in the 21st century in the Goddard Earth Observing System Chemistry-Climate Model (GEOSCCM). *Journal of Geophysical Research*, 117(D20), D20119. <https://doi.org/10.1029/2012JD017905>
- Li, Y., An, W., Pang, H., Wu, S., Tang, Y., Zhang, W., & Hou, S. (2020). Variations of stable isotopic composition in atmospheric water vapor and their controlling factors – A six-year continuous sampling study in Nanjing, eastern China. *Journal of Geophysical Research: Atmospheres*, 125(22), e2019JD031697. <https://doi.org/10.1029/2019JD031697>
- Liu, K., Hou, S., Wu, S., Pang, H., Zhang, W., Song, J., et al. (2021). The atmospheric iron variations during 1950–2016 recorded in snow at Dome Argus, East Antarctica. *Atmospheric Research*, 248, 105263. <https://doi.org/10.1016/j.atmosres.2020.105263>
- Luz, B., & Barkan, E. (2010). Variations of  $^{17}\text{O}/^{16}\text{O}$  and  $^{18}\text{O}/^{16}\text{O}$  in meteoric waters. *Geochimica et Cosmochimica Acta*, 74(22), 6276–6286. <https://doi.org/10.1016/j.gca.2010.08.016>
- Lyons, J. R. (2001). Transfer of mass-independent fractionation in ozone to other oxygen-containing radicals in the atmosphere. *Geophysical Research Letters*, 28(17), 3231–3234. <https://doi.org/10.1029/2000gl012791>
- Lyons, J. R. (2003). Mass-independent fractionation in stratospheric water: A potential new indicator of provenance. *Geophysical Research Abstracts*, 5, 13565.
- Marshall, G. J. (2003). Trends in the Southern Annular Mode from observations and reanalyses. *Journal of Climate*, 16(24), 4134–4143. [Dataset]. [https://doi.org/10.1175/1520-0442\(2003\)016<4134:titsam>2.0.co;2](https://doi.org/10.1175/1520-0442(2003)016<4134:titsam>2.0.co;2)
- Matthes, K., Langematz, U., Gray, L. L., Koder, K., & Labitzke, K. (2004). Improved 11-year solar signal in the Freie Universität Berlin Climate Middle Atmosphere Model (FUB-CMAM). *Journal of Geophysical Research*, 109(D6), D06101. <https://doi.org/10.1029/2003JD004012>
- Mauersberger, K., Krankowsky, D., & Janssen, C. H. (2003). Oxygen isotope processes and transfer reactions. *Space Science Reviews*, 106(1/4), 265–279. <https://doi.org/10.1023/a:1024650007258>
- Mauersberger, K., Lämmerzahl, P., & Krankowsky, D. (2001). Stratospheric ozone isotope enrichments-revisited. *Geophysical Research Letters*, 28(16), 3155–3158. <https://doi.org/10.1029/2001gl013439>
- Miller, M. F. (2008). Comment on “Record of  $\delta^{18}\text{O}$  and  $^{17}\text{O}$ -excess in ice from Vostok Antarctica during the last 150,000 years” by Amaelle Landais et al. *Geophysical Research Letters*, 35(23), L23709. <https://doi.org/10.1029/2008gl034505>
- Miller, M. F. (2018). Precipitation regime influence on oxygen triple-isotope distributions in Antarctic precipitation and ice cores. *Earth and Planetary Science Letters*, 481, 316–327. <https://doi.org/10.1016/j.epsl.2017.10.035>
- Naik, S. S., Thamban, M., Laluraj, C. M., Redkar, B. L., & Chaturvedi, A. (2010). A century of climate variability in central Dronning Maud Land, East Antarctica, and its relation to Southern Annual Mode and El Niño-Southern Oscillation. *Journal of Geophysical Research*, 115(16), D16102–D16113. <https://doi.org/10.1029/2009jd013268>
- Pang, H., Hou, S., Landais, A., Masson-Delmotte, V., Jouzel, J., Steen-Larsen, H. C., et al. (2019). Influence of Summer Sublimation on  $\delta\text{D}$ ,  $\delta^{18}\text{O}$ , and  $\delta^{17}\text{O}$  in precipitation, East Antarctica, and Implications for Climate Reconstruction From Ice Cores. *Journal of Geophysical Research: Atmospheres*, 124, 7339–7358. <https://doi.org/10.1029/2018jd030218>
- Pang, H., Hou, S., Landais, A., Masson-Delmotte, V., Prie, F., Steen-Larsen, H. C., et al. (2015). Spatial distribution of  $^{17}\text{O}$ -excess in surface snow along a traverse from Zhongshan station to Dome A, East Antarctica. *Earth and Planetary Science Letters*, 44, 126–133. <https://doi.org/10.1016/j.epsl.2015.01.014>
- Pang, H., Zhang, P., Wu, S., Jouzel, J., Steen-Larsen, H. C., Liu, K., et al. (2022).  $^{17}\text{O}$ -excess data of two snow pits at Dome A [Dataset]. Zenodo. <https://doi.org/10.5281/zenodo.6470612>

- Ploeger, F., Legras, B., Charlesworth, E., Yan, X., Diallo, M., Konopka, P., et al. (2019). How robust are stratospheric age of air trends from different reanalyses? *Atmospheric Chemistry and Physics*, 19(9), 6085–6105. <https://doi.org/10.5194/acp-19-6085-2019>
- Risi, C., Landais, A., Bony, S., Jouzel, J., Masson-Delmotte, V., & Vimeux, F. (2010). Under-standing the  $^{17}\text{O}$ -excess glacial-interglacial variations in Vostok precipitation. *Journal of Geophysical Research*, 115(D10), D10112. <https://doi.org/10.1029/2008JD011535>
- Risi, C., Landais, A., Winkler, R., & Vimeux, F. (2013). Can we determine what controls the spatio-temporal distribution of d-excess and  $^{17}\text{O}$ -excess in precipitation using the LMDZ general circulation model? *Climate of the Past*, 9(5), 2173–2193. <https://doi.org/10.5194/cp-9-2173-2013>
- Roscoe, H. K. (2004). Possible descent across “Tropopause” in Antarctic winter. *Advances in Space Research*, 33(7), 1048–1052. [https://doi.org/10.1016/s0273-1177\(03\)00587-8](https://doi.org/10.1016/s0273-1177(03)00587-8)
- Schneider, D. P., Steig, E. J., van Ommen, T. D., Dixon, D. A., Mayewski, P. A., Jones, J. M., & Bitz, C. M. (2006). Antarctic temperatures over the past two centuries from ice cores. *Geophysical Research Letters*, 33(16), L16707–L16711. <https://doi.org/10.1029/2006gl027057>
- Schoenemann, S. W., & Steig, E. J. (2016). Seasonal and spatial variations of  $^{17}\text{O}$ -excess and decess in Antarctic precipitation: Insights from an intermediate complexity isotope model. *Journal of Geophysical Research: Atmospheres*, 121(19), 11215–11247. <https://doi.org/10.1002/2016jd025117>
- Schoenemann, S. W., Steig, E. J., Ding, Q., Markle, B. R., & Schauer, A. J. (2014). Triple water-isotopologue record from WAIS Divide, Antarctica: Controls on glacial-interglacial changes in  $^{17}\text{O}$ -excess of precipitation. *Journal of Geophysical Research: Atmospheres*, 119(14), 8741–8763. <https://doi.org/10.1002/2014JD021770>
- Schueler, B., Morton, J., & Mauersberger, K. (1990). Measurement of isotopic abundances in collected stratospheric ozone samples. *Geophysical Research Letters*, 17(9), 1295–1298. <https://doi.org/10.1029/gl017i009p01295>
- Shi, C., Cai, J., Guo, D., Xu, T., & Lu, Y. (2018). Responses of stratospheric temperature and Brewer-Dobson circulation to 11-year solar cycle in boreal winter. *Transactions of Atmospheric Sciences*, 41(2), 275–281. (in Chinese).
- Steen-Larsen, H. C., Masson-Delmotte, V., Hirabayashi, M., Winkler, R., Satow, K., Prie, F., et al. (2014). What controls the isotopic composition of Greenland surface snow? *Climate of the Past*, 10(1), 377–392. <https://doi.org/10.5194/cp-10-377-2014>
- Tang, Y., Pang, H., Zhang, W., Li, Y., Wu, S., & Hou, S. (2015). Effects of changes in moisture source and the upstream rainout on stable isotopes in precipitation – A case study in Nanjing, eastern China. *Hydrology and Earth System Sciences*, 19(10), 4293–4306. <https://doi.org/10.5194/hess-19-4293-2015>
- Thiemens, M. H. (1999). Mass-independent isotope effects in planetary atmospheres and the early solar system. *Science*, 283(5400), 341–345. <https://doi.org/10.1126/science.283.5400.341>
- Thiemens, M. H. (2006). History and applications of mass-independent isotope effects. *Annual Review of Earth and Planetary Sciences*, 34(1), 217–262. <https://doi.org/10.1146/annurev.earth.34.031405.125026>
- Touzeau, A., Landais, A., Stenni, B., Uemura, R., Fukui, K., Fujita, S., et al. (2016). Acquisition of isotopic composition for surface snow in East Antarctica and the links to climatic parameters. *The Cryosphere*, 10(2), 837–852. <https://doi.org/10.5194/tc-10-837-2016>
- Uppala, S. M., K  llberg, P. W., Simmons, A. J., Andrae, U., Da Costa Bechtold, V., Fiorino, M., et al. (2005). The ERA-40 re-analysis. Quarterly Journal of the Royal Meteorological Society, 131(612), 2961–3012. [Dataset]. <https://apps.ecmwf.int/datasets/data/era40-daily/levtype=sfc/>
- WDC-SILSO, Royal Observatory of Belgium, Brussels. Royal Observatory of Belgium. WDCSILSO, [Dataset]. Retrieved from <https://www.wbis.sidc.be/silso/datafiles>
- Winkler, R., Landais, A., Risi, C., Baroni, M., Ekaykin, A., Jouzel, J., et al. (2013). Interannual variation of water isotopologues at Vostok indicates a contribution from stratospheric water vapour. *Proceedings of the National Academy of Sciences of the United States of America*, 110(44), 17674–17679. <https://doi.org/10.1073/pnas.1215209110>
- Winkler, R., Landais, A., Sodemann, H., D  mbgen, L., Pri  , F., Masson-Delmotte, V., et al. (2012). Deglaciation records of  $^{17}\text{O}$ -excess in East Antarctica: Reliable reconstruction of oceanic normalized relative humidity from coastal sites. *Climate of the Past*, 8(1), 1–16. <https://doi.org/10.5194/cp-8-1-2012>
- Zahn, A., Franz, P., Bechtel, C., Gro  , J. U., & R  ckmann, T. (2006). Modeling the budget of middle atmospheric water vapour isotopes. *Atmospheric Chemistry and Physics*, 6(8), 2073–2090. <https://doi.org/10.5194/acp-6-2073-2006>

## References From the Supporting Information

- Andrews, D., Holton, J., & Leovy, C. (1987). *Middle atmosphere dynamics*. Academic Press.
- Barkan, E., & Luz, B. (2007). Diffusivity fractionations of  $\text{H}_2^{16}\text{O}/\text{H}_2^{17}\text{O}$  and  $\text{H}_2^{16}\text{O}/\text{H}_2^{18}\text{O}$  in air and their implications for isotope hydrology. *Rapid Communications in Mass Spectrometry*, 21(18), 2999–3005. <https://doi.org/10.1002/rcm.3180>
- Chen, D. (1995). A residual circulation derived from an energy balance climate model. *Journal of Geophysical Research*, 100(D10), 21137. <https://doi.org/10.1029/95jd02033>
- Edmon, H. J., Hoskins, B. J., & McIntyre, M. E. (1980). Eliassen-Palm cross-sections for the troposphere. *Journal of the Atmospheric Sciences*, 37(12), 2600–2616. [https://doi.org/10.1175/1520-0469\(1980\)037<2600:epsft>2.0.co;2](https://doi.org/10.1175/1520-0469(1980)037<2600:epsft>2.0.co;2)
- Ekaykin, A. A. (2003). *Meteorological regime of central Antarctica and its role in the formation of isotope composition of snow thickness*, These Doctorat de l’Universite Joseph Fourier. (p. 136).
- Elle  h  j, M. D., Steen-Larsen, H. C., Johnsen, S. J., & Madsen, M. B. (2013). Ice-vapor equilibrium fractionation factor of hydrogen and oxygen isotopes: Experimental investigations and implications for stable water isotope studies. *Rapid Communications in Mass Spectrometry*, 27(19), 2149–2158. <https://doi.org/10.1002/rcm.6668>
- Holton, J. R. (1990). On the global exchange of mass between the stratosphere and troposphere. *Journal of the Atmospheric Sciences*, 47(3), 392–395. [https://doi.org/10.1175/1520-0469\(1990\)047<0392:otgeom>2.0.co;2](https://doi.org/10.1175/1520-0469(1990)047<0392:otgeom>2.0.co;2)
- Horita, J., & Wesolowski, D. (1994). Liquid-vapor fractionation of oxygen and hydrogen isotopes of water from the freezing to the critical temperature. *Geochimica et Cosmochimica Acta*, 58(16), 3425–3437. [https://doi.org/10.1016/0016-7037\(94\)90096-5](https://doi.org/10.1016/0016-7037(94)90096-5)
- Luz, B., Barkan, E., Yam, R., & Shemesh, A. (2009). Fractionation of oxygen and hydrogen isotopes in evaporating water. *Geochimica et Cosmochimica Acta*, 73(22), 6697–6703. <https://doi.org/10.1016/j.gca.2009.08.008>
- Rind, D., Chandler, M., Lonergan, P., & Lerner, J. (2001). Climate change and the middle atmosphere: 5. Paleostratosphere in cold and warm climates. *Journal of Geophysical Research*, 106(D17), 20195–20212. <https://doi.org/10.1029/2000jd900548>
- Wang, Y., Sodemann, H., Hou, S., Masson-Delmotte, V., Jouzel, J., & Pang, H. (2013). Snow accumulation and its moisture origin over Dome Argus, Antarctica. *Climate Dynamics*, 40(3–4), 731–742. <https://doi.org/10.1007/s00382-012-1398-9>
- WMO. (1992). *International meteorological vocabulary*, Genf. (p. 784).